

Periacetabular Osteotomy Restores the Typically Excessive Range of Motion in Dysplastic Hips With a Spherical Head

Simon D. Steppacher MD, Corinne A. Zurmühle MD, Marc Puls PhD,
Klaus A. Siebenrock MD, Michael B. Millis MD, Young-Jo Kim MD, PhD,
Moritz Tannast MD

© The Association of Bone and Joint Surgeons® 2014

Abstract

Background Residual acetabular dysplasia is seen in combination with femoral pathomorphologies including an aspherical femoral head and valgus neck-shaft angle with high antetorsion. It is unclear how these femoral pathomorphologies affect range of motion (ROM) and impingement zones after periacetabular osteotomy.

Questions/purposes (1) Does periacetabular osteotomy (PAO) restore the typically excessive ROM in dysplastic hips compared with normal hips; (2) how do impingement locations differ in dysplastic hips before and after PAO compared with normal hips; (3) does a concomitant cam-type morphology adversely affect internal rotation; and

(4) does a concomitant varus-derotation intertrochanteric osteotomy (IO) affect external rotation?

Methods Between January 1999 and March 2002, we performed 200 PAOs for dysplasia; of those, 27 hips (14%) met prespecified study inclusion criteria, including availability of a pre- and postoperative CT scan that included the hip and the distal femur. In general, we obtained those scans to evaluate the pre- and postoperative acetabular and femoral morphology, the degree of acetabular reorientation, and healing of the osteotomies. Three-dimensional surface models based on CT scans of 27 hips before and after PAO and 19 normal hips were created. Normal hips were obtained from a population of CT-based computer-assisted THAs using the contralateral hip after exclusion of symptomatic hips or hips with abnormal radiographic anatomy. Using validated and computerized methods, we then determined ROM (flexion/extension, internal- [IR]/external rotation [ER], adduction/abduction) and two motion patterns including the anterior (IR in flexion) and posterior (ER in extension) impingement tests. The computed impingement locations were assigned to anatomical locations of the pelvis and the femur. ROM was calculated separately for hips with ($n = 13$) and without ($n = 14$) a cam-type morphology and PAOs with ($n = 9$) and without ($n = 18$) a concomitant IO. A post hoc power analysis based on the primary research question with an alpha of 0.05 and a beta error of 0.20 revealed a minimal detectable difference of 4.6° of flexion.

Results After PAO, flexion, IR, and adduction/abduction did not differ from the nondysplastic control hips with the numbers available (p ranging from 0.061 to 0.867). Extension was decreased ($19^\circ \pm 15^\circ$; range, -18° to 30° versus $28^\circ \pm 3^\circ$; range, 19° – 30° ; $p = 0.017$) and ER in 0° flexion was increased ($25^\circ \pm 18^\circ$; range, -10° to 41° versus $38^\circ \pm 7^\circ$; range, 17° – 41° ; $p = 0.002$). Dysplastic hips had a

One author (MT) has received funding from the Swiss National Science Foundation (SNSF).

All ICMJE Conflict of Interest Forms for authors and *Clinical Orthopaedics and Related Research*® editors and board members are on file with the publication and can be viewed on request.

Clinical Orthopaedics and Related Research® neither advocates nor endorses the use of any treatment, drug, or device. Readers are encouraged to always seek additional information, including FDA-approval status, of any drug or device prior to clinical use.

Each author certifies that his or her institution approved the human protocol for this investigation, that all investigations were conducted in conformity with ethical principles of research, and that informed consent for participation in the study was obtained.

S. D. Steppacher (✉), C. A. Zurmühle, M. Puls,
K. A. Siebenrock, M. Tannast
Department of Orthopaedic Surgery, Inselspital, University
of Bern, Freiburgstrasse, 3010 Bern, Switzerland
e-mail: simon.steppacher@insel.ch

M. B. Millis, Y.-J. Kim
Department of Orthopaedic Surgery, Boston Children's Hospital,
Harvard Medical School, Boston, MA, USA

higher prevalence of extraarticular impingement at the anteroinferior iliac spine compared with normal hips (48% [13 of 27 hips] versus 5% [one of 19 hips], $p = 0.002$). A PAO increased the prevalence of impingement for the femoral head from 30% (eight of 27 hips) preoperatively to 59% (16 of 27 hips) postoperatively ($p = 0.027$). IR in flexion was decreased in hips with a cam-type deformity compared with those with a spherical femoral head (p values from 0.002 to 0.047 for 95° – 120° of flexion). A concomitant IO led to a normalization of ER in extension (eg, $37^\circ \pm 7^\circ$ [range, 21° – 41°] of ER in 0° of flexion in hips with concomitant IO compared with $38^\circ \pm 7^\circ$ [range, 17° – 41°] in nondysplastic control hips; $p = 0.777$).

Conclusions Using computer simulation of hip ROM, we could show that the PAO has the potential to restore the typically excessive ROM in dysplastic hips. However, a PAO can increase the prevalence of secondary intraarticular impingement of the aspherical femoral head and extraarticular impingement of the anteroinferior iliac spines in flexion and internal rotation. A cam-type morphology can result in anterior impingement with restriction of IR. Additionally, a valgus hip with high antetorsion can result in posterior impingement with decreased ER in extension, which can be normalized with a varus derotation IO of the femur. However, indication of an additional IO needs to be weighed against its inherent morbidity and possible complications. The results are based on a limited number of hips with a pre- and postoperative CT scan after PAO. Future prospective studies are needed to verify the current results based on computer simulation and to test their clinical importance.

Level of Evidence Level III, therapeutic study.

Introduction

Patients with developmental dysplasia of the hip (DDH) often have proximal femoral deformities [15, 22, 23]. Frequently found femoral pathomorphologies with DDH are an aspherical femoral head [21] and a valgus neck-shaft angle with high antetorsion [15, 23]. The aspherical femoral head may result in symptomatic secondary cam-type impingement, which can compromise internal rotation (IR) in flexion after acetabular reorientation [1]. The valgus morphology with high femoral antetorsion can lead to painful restricted external rotation (ER) in extension as a result of a posterior impingement [11, 28]. Referring to these two femoral pathomorphologies, ROM in DDH after periacetabular osteotomy (PAO) can potentially be addressed with offset correction or an intertrochanteric osteotomy (IO). However, ROM after PAO has not been quantified using objective methods.

Objective quantification of the osseous ROM of the hip can be achieved with CT-based virtual simulations. To simulate ROM for complex deformities (such as DDH), classic motion algorithms with a single center of rotation have been shown to be unreliable [18]. The “Equidistant Method” [18] has been presented to solve this issue. It is reportedly superior to previously presented motion algorithms [18]. This validated algorithm continuously adjusts the hip center based on the morphology of the articulating surfaces of the femoral head and the acetabulum. This technique has been successfully applied to detect ROM in hips with more complex deformities including femoro-acetabular impingement [7, 25], valgus hips with high antetorsion [20], and Legg-Calvé-Perthes disease [24].

We used this method to quantify ROM after PAO and to evaluate the effect of an additional cam-type deformity or IO. We questioned (1) if a PAO restores the typically excessive ROM in dysplastic hips compared with normal hips; (2) how impingement locations differ in dysplastic hips before and after PAO compared with normal hips; (3) if a cam-type morphology of the proximal femur negatively affects IR in flexion after PAO; and (4) how a concomitant varus derotation IO affects ER in extension after PAO when a valgus morphology of the proximal femur with high antetorsion was present preoperatively.

Patients and Methods

In a retrospective comparative study, we compared the pre- and postoperative ROM of symptomatic patients undergoing PAO for DDH with the hip ROM in normal hips. Between January 1999 and March 2002 a total of 165 patients (200 hips) underwent PAO for symptomatic DDH at the institution of two coauthors (MBM, Y-JK). Inclusion criteria were the availability of both a pre- and postoperative pelvic CT scans. A preoperative CT scan was performed in the majority of patients (131 of 165 patients and 156 hips [78%]) for preoperative evaluation of acetabular morphology, femoral version, and three-dimensional surgical planning. Not all patients had a preoperative CT scan as a result of the steadily increasing number of patients with a preoperative MRI in this time period offering the advantage of decreased radiation exposure, evaluation of both the acetabular and the femoral morphology, and assessment of labral and chondral degeneration. A postoperative CT scan was performed in a minority of 58 patients (70 hips) for visualization of the postoperative acetabular coverage, assessment of femoral torsion, or evaluation of bony union of the osteotomies. Both a pre- and postoperative CT scan were performed in 48 patients (58 hips). Exclusion criteria were CT scans not including the distal part of the femur (impeding the quantification of femoral torsion; 12 hips), with insufficient slice

Table 1. Demographic and radiographic data of the three study groups*

Parameter	Dysplasia (preoperatively)	Dysplasia (after PAO)	Normal	p value preoperative versus PAO	p value preoperative versus normal	p value PAO versus normal
Number of patients	20	20	19	–	–	–
Number of hips	27	27	19	–	–	–
Age (years)	–	27 ± 10 (13–44)	54 ± 11 (31–73)	–	–	< 0.001
Sex (percent male of all hips)	11	11	53	1.000	0.003	0.003
Side (percent right of all hips)	59	59	26	1.000	0.038	0.038
Lateral center-edge angle (°)	1 ± 15 (–44 to 17)	36 ± 6 (27–46)	31 ± 4 (25–37)	< 0.001	< 0.001	0.007
Acetabular index (°)	27 ± 7 (11–39)	1 ± 6 (–17 to 12)	7 ± 3 (0–12)	< 0.001	< 0.001	0.001
Extrusion index (°)	48 ± 14 (33–86)	15 ± 6 (7–28)	23 ± 5 (12–33)	< 0.001	< 0.001	< 0.001
Total acetabular coverage (percent)	50 ± 17 (6–71)	87 ± 8 (69–100)	80 ± 7 (68–93)	< 0.001	< 0.001	0.002
Anterior acetabular coverage (percent)	7 ± 4 (0–13)	10 ± 5 (2–23)	21 ± 5 (13–28)	0.009	< 0.001	< 0.001
Posterior acetabular coverage (percent)	30 ± 12 (6–54)	57 ± 11 (35–81)	49 ± 8 (37–63)	< 0.001	< 0.001	0.008
Crossover sign (percent positive)	22	0	0	0.023	< 0.001	0.413
Retroversion index (percent positive) [†]	21 ± 10 (10–34)	–	–	–	–	–
Posterior wall sign (percent positive)	93	11	11	< 0.001	< 0.001	1.000
Alpha angle (°)	50 ± 10 (27–69)	–	42 ± 4 (36–50)	–	< 0.002	–
Centrum collum diaphyseal angle (°)	140 ± 7 (128–158)	135 ± 6 (119–144)	130 ± 4 (123–137)	0.007	< 0.001	0.002
Femoral antetorsion (°)	39 ± 13 (10–62)	28 ± 14 (2–55)	19 ± 7 (7–39)	0.325	0.030	0.047

Values are expressed as mean ± SD with range in parentheses; *description of the radiographic parameters in Tannast M, Siebenrock KA, Anderson SE. Femoroacetabular impingement: radiographic diagnosis—what the radiologist should know. *AJR Am J Roentgenol.* 2007;188:1540–1552; [†]only in hips with a positive retroversion sign; PAO = periacetabular osteotomy.

thickness > 3 mm for the computer simulation (10 hips), and without or incomplete hardware removal (seven hips), or a THA of the contralateral side (two hips) resulting in metal artefact. This resulted in 20 patients (27 hips [14%]) for evaluation (dysplasia group; Table 1). These hips in the dysplasia group did not differ from the 145 excluded patients (173 hips) in terms of age at operation (27 ± 10 years; range, 13–44 years versus 27 ± 11 years; range, 10–49 years, $p = 0.926$), gender (11% [three of 27 hips] versus 18% [32 of 173 hips] male; $p = 0.427$), and side (59% [16 of 27 hips] versus 54% [93 of 173 hips] right, $p = 0.680$). The PAOs were performed according to the original technique described by Ganz et al. [3] (PAO group). In nine of 27 hips (33%) a concomitant IO was performed. There was one isolated derotational osteotomy and a combined varus derotational osteotomy in eight hips. The indication for the IO was a positive posterior apprehension test (painful extension and ER) associated with a centrum collum diaphyseal (CCD) angle of more than 135° [28] and/or femoral antetorsion

exceeding 25° [9]. No arthrotomy with offset correction was performed. The normal hips were selected from the contralateral hips of 146 patients undergoing CT-based computer-assisted THA. Hips with the following features were excluded: osteoarthritis ≥ Grade 1 according to Tönnis and Heinecke [28] (40 hips), lateral center-edge angle of less than 25° (24 hips), a pistol grip deformity [4] (13 hips), coxa profunda [27] (13 hips), THA or TKA (10 hips), incomplete radiographic documentation (eight hips), alpha angle [16] > 50° (four hips), acetabular retroversion [19] (four hips), pain (four hips), previous hip surgery (three hips), protrusio acetabuli [27] (two hips), femoral retrotorsion (one hip), and coxa valga (one hip). Eventually, the normal group consisted of 19 patients (19 hips; Table 1). The study was approved by the local institutional review board.

The pelvic CT scans imaged the hips including the antero-inferior iliac spine and the distal part of the femur. The pixel spacing ranged from 0.586 to 0.938 mm/pixel with a constant interslice distance from 3 mm. Based on the CT

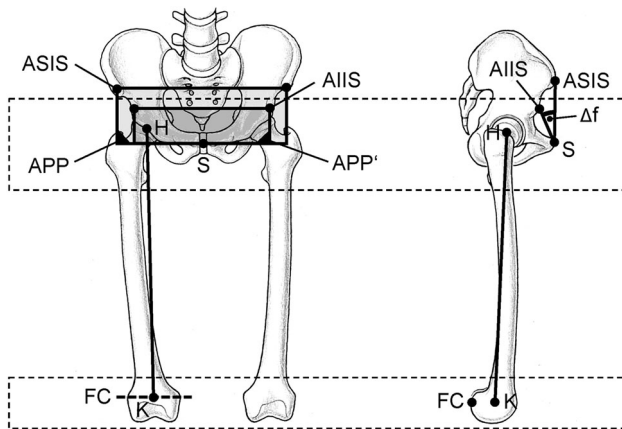


Fig. 1 The definitions of the pelvic or femoral anatomical coordinate systems used to simulate hip ROM are as follows: the anterior pelvic plane (APP) is defined by the ASISs and the pubic tubercles. To minimize radiation exposure, the anterior superior iliac spines (ASISs) were not always covered in the CT. The APP was therefore reconstructed using a plane formed by the inferior iliac spines and the pubic tubercles and a tilt angle of 20° [25]. The femoral coordinate system was defined by the axis through the femoral head (H) and the center of the knee (K). The femoral condyles (FC) were used as rotational reference. Reprinted and adapted with permission from John Wiley and Sons: Tannast M, Kubiak-Langer M, Langlotz F, Puls M, Murphy SB, Siebenrock KA. Noninvasive three-dimensional assessment of femoroacetabular impingement. *J Orthop Res.* 2007;25:122–131, Figure 3. Copyright © 2006 Orthopaedic Research Society.

scan, three-dimensional (3-D) surface models of the pelvis and femur were computed semiautomatically using Amira visualization software (Version 5.4; Visage Imaging Inc, Carlsbad, CA, USA). Femoral and pelvic reference coordinate systems were defined for hip ROM simulation. The femoral coordinate system was defined by the hip and the knee centers and the posterior aspects of the femoral condyles (Fig. 1) [9, 25]. The anterior pelvic plane (APP) was used as the pelvic reference coordinate system, which is defined by the anterosuperior iliac spines (ASISs) and the pubic tubercles. To minimize radiation exposure, the ASISs were not always imaged in the CT. The APP was therefore reconstructed using a plane formed by the inferior iliac spines and the pubic tubercles and a tilt angle of 20° [26].

Specifically designed and previously validated software to simulate ROM was applied to each hip of the three study groups [25]. Input data included the previously generated 3-D femur and pelvis models. The software uses a fully automated algorithm for detection of the acetabular rim [17], a best-fitting sphere algorithm to define the center of the femoral head and acetabulum [8], and the Equidistant Method for motion analysis [18]. The Equidistant Method is an algorithm with a dynamic hip center, which allows simulated ROM and impingement detection more accurately than other motion algorithms, eg, with a fixed center of rotation [18]. This algorithm calculates ROM stepwise in 1°

increments. For each 1° step, the contact surfaces of the femur and the acetabulum are reconstructed. These surfaces are used to construct the best-fitting spheres (one femoral and one acetabular). To adjust for joint irregularities, the centers of rotation of these two spheres are then matched [18]. Cadaver validation of the Equidistant Method showed a mean error of ROM of $2.6^\circ \pm 2.5^\circ$ and a mean error to localize the osseous impingement of $1.3 \text{ mm} \pm 1.2 \text{ mm}$ [18]. A good to excellent reproducibility (intraclass correlation coefficient [ICC] ranging from 0.88 to 0.99) was found for all modalities of ROM [26]. Reliability was good to excellent (ICC ranging from 0.87 to 0.95) for all modalities except ER (ICC of 0.48) [25].

For the primary research question, we compared ROM including flexion, extension, IR in 90° of flexion, ER in 0° of flexion, abduction, and adduction between dysplastic hips before and after PAO and in comparison to the normal group. In addition, two established motion patterns corresponding to the anterior and posterior impingement test were evaluated [20, 24, 25]. For the anterior impingement test, flexion was evaluated in 1° increments between 90° and 120° of flexion and -10° and 40° of IR. For the posterior impingement test, extension was evaluated in 1° increments between -20° and 10° of extension and 0° and 50° of ER.

For the second research question, the computed impingement locations for the two motion patterns were assigned to anatomical locations of the pelvis and the femur analogous to previously published motion analyses [20, 24]. The possible pelvic impingement areas were divided into: acetabular rim, lunate surface, anteroinferior iliac spine, supraacetabular, and ischium. The possible femoral impingement areas were divided into: femoral head, femoral neck, femoral head-neck junction, greater and lesser trochanter, intertrochanteric crest, and femoral shaft.

For the third research question, the anterior impingement test was compared between PAOs with (13 hips) and without a cam-type deformity (14 hips). A cam-type deformity was defined by an alpha angle exceeding 50° on the radial CT reconstructions of the head-neck area in the anterosuperior quadrant (from 12 to 3 o'clock) [16]. The acetabular reorientation did not differ between hips with and without a cam-type deformity (Table 2).

For the fourth research question, the posterior impingement test motion pattern was compared between PAOs with (9 hips) and without a concomitant IO (18 hips). Preoperatively, hips with a planned PAO and concomitant IO had an increased CCD angle ($145^\circ \pm 7^\circ$; range, 135° – 158° versus $138^\circ \pm 5^\circ$; range, 128° – 150° ; $p = 0.021$) and femoral ante-torsion ($53^\circ \pm 11^\circ$; range, 31° – 68° versus $38^\circ \pm 11^\circ$; range, 13° – 57° ; $p = 0.005$) compared with hips undergoing PAO only. The postoperative acetabular reorientation did not differ between hips with and without an IO (Table 2).

Table 2. Acetabular and femoral anatomy of hips after PAO with and without a cam-type morphology or with and without an IO

Parameter	PAO without cam-type morphology (n = 14)	PAO with cam-type morphology (n = 13)	p value without versus with cam	PAO without IO (n = 18)	PAO with IO (n = 9)	p value without versus with IO
Acetabular anatomy						
Lateral center-edge angle (°)	37 ± 7 (27–52)	36 ± 7 (25–46)	0.627	38 ± 7 (27–58)	36 ± 8 (25–52)	0.520
Acetabular index (°)	1 ± 7 (–17 to 12)	2 ± 6 (–6 to 15)	0.847	1 ± 6 (–17 to 12)	2 ± 7 (–7 to 15)	0.979
Extrusion index (percent)	14 ± 5 (8–23)	16 ± 6 (7–28)	0.771	14 ± 5 (7–24)	15 ± 7 (8–28)	0.837
Total acetabular coverage (percent)	89 ± 7 (78–100)	85 ± 8 (69–96)	0.610	87 ± 7 (74–96)	87 ± 10 (69–100)	0.959
Anterior acetabular coverage (percent)	10 ± 6 (2–23)	10 ± 5 (2–19)	0.560	10 ± 5 (2–19)	10 ± 6 (2–23)	0.817
Posterior acetabular coverage (percent)	55 ± 14 (35–81)	59 ± 7 (44–70)	0.167	58 ± 10 (36–78)	55 ± 14 (35–81)	0.537
Retroversion sign (percent positive)	0	0	1.000	0	0	1.000
Posterior wall sign (percent positive)	21	0	0.222	11	11	1.000
Femoral anatomy						
Alpha angle (°)	42 ± 6 (27–49)	58 ± 6 (51–69)	< 0.001	53 ± 9 (39–69)	44 ± 10 (27–61)	0.037
Centrum collum diaphyseal angle	134 ± 4 (126–139)	135 ± 7 (119–144)	0.593	137 ± 3 (130–144)	130 ± 6 (119–139)	0.012
Femoral antetorsion (°)	28 ± 15 (8–55)	27 ± 12 (2–49)	0.923	38 ± 11 (11–57)	5 ± 16 (–29–23)	< 0.001

Values are expressed as mean ± SD with ranges in parentheses; PAO = periacetabular osteotomy; IO = intertrochanteric osteotomy.

The Kolmogorov-Smirnov test was used to test for normal distribution. Because not all parameters showed normal distribution, only nonparametric tests were used. ROM, anterior and posterior impingement motion patterns, and demographic or radiographic data were compared between the dysplasia and the PAO groups using the Wilcoxon test and between the normal group and the dysplasia or PAO group, respectively, using the Mann-Whitney U test. The subgroups of PAO (with and without cam, with and without IO) were compared using the Mann-Whitney U test. Binominal demographic data were compared using the Fisher's exact test. As a result of the limited number of hips included in the study groups we performed a post hoc power analysis to determine the minimal detectable difference. This power analysis was performed based on the primary research question (difference in flexion between dysplastic hips and hips after PAO) and with the following parameters: alpha error 0.05, beta error 0.2, group size of 27 hips (Table 1), mean flexion of 148° (Table 3), and a SD of 20° of flexion (Table 3). This resulted in a minimal detectable difference of 4.6°.

Results

In dysplastic hips after PAO, the following amplitudes of ROM (Table 3) were decreased compared with preoperatively: flexion ($127^\circ \pm 19^\circ$; range, 84° – 161° versus $148^\circ \pm 20^\circ$; range, 97° – 171° ; $p < 0.001$) and abduction ($57^\circ \pm 14^\circ$; range, 22° – 75° versus $88^\circ \pm 4^\circ$; range, 73° – 90° ; $p < 0.001$). In contrast, adduction ($48^\circ \pm 14^\circ$; range, 7° – 61° versus $41^\circ \pm 13^\circ$; range, 5° – 61° ; $p = 0.029$) was increased in dysplastic hips after PAO compared with preoperatively (Table 3). Comparing ROM in dysplastic hips after PAO with the normal group extension ($19^\circ \pm 15^\circ$; range, -18° to 30° versus $28^\circ \pm 3^\circ$; range, 19° – 30° ; $p = 0.017$) and ER in 0° of flexion ($25^\circ \pm 18^\circ$; range, -10° to 41° versus $38^\circ \pm 7^\circ$; range, 17° – 41° ; $p = 0.002$) were decreased. No differences were observed for flexion, IR in 90° of flexion, adduction, and abduction (p ranging from 0.061 to 0.867) between dysplastic hips after PAO and the normal control hips with the numbers available (Table 3). For the anterior impingement test, there was no difference for IR between dysplastic hips after PAO and normal control hips with the number available (p ranging from 0.151 to 0.902; Fig. 2A). For the posterior impingement test, dysplastic hips after PAO had decreased ER compared with the normal control hips with the numbers available (p ranging from 0.001 to 0.018; Fig. 2C).

For the anterior impingement motion pattern, dysplastic hips had a higher prevalence of impingement for the antero-inferior iliac spine (48% [13 of 27 hips] versus 5% [one

of 19 hips], $p = 0.002$; Fig. 3A) in comparison to normal hips (Table 4). A lower prevalence of impingement was found for the acetabular rim (78% [21 of 27 hips] versus 100% [19 of 19 hips], $p = 0.032$; Table 4). A PAO resulted in a higher prevalence of femoral head impingement compared with the native dysplastic hip (59% [16 of 27 hips] versus 30% [eight of 27 hips], $p = 0.027$; Table 4, Fig. 3B). For the posterior impingement pattern, dysplastic hips had a higher prevalence of impingement for the lunate surface (44% [12 of 27 hips] versus 0% [zero of 19 hips], $p < 0.001$; Fig. 3C), greater trochanter (19% [five of 27 hips] versus 0% [zero of 19 hips], $p = 0.059$), and femoral neck (26% [seven of 27 hips] versus 0% [zero of 19 hips], $p = 0.017$) in comparison to normal hips (Fig. 3D). A lower prevalence was found for the acetabular rim (22% [six of 27 hips] versus 84% [16 of 19 hips], $p < 0.001$) and the femoral head-neck junction (22% [six of 27 hips] versus 79% [15 of 19 hips], $p < 0.001$). A PAO resulted in a higher prevalence of impingement for the greater trochanter (59% [16 of 27 hips] versus 19% [five of 27 hips], $p = 0.002$) and a lower prevalence for the femoral neck (4% [one of 27 hips] versus 26% [seven of 27 hips], $p = 0.025$) compared with the native dysplastic hip (Table 4).

After PAO, hips with a cam-type morphology of the proximal femur had decreased IR from 95° to 120° of flexion compared with hips with a spherical head-neck morphology (p ranging from 0.002 to 0.047; Fig. 2B); eg, IR at 110° of flexion was decreased in hips with a cam-type morphology ($13^\circ \pm 22^\circ$; range, -20° to 39°) compared with hips with a spherical head-neck morphology ($33^\circ \pm 14^\circ$; range, -7° to 41°); $p = 0.002$; Fig. 2B). In addition, IR was increased in hips with a spherical head-neck morphology compared with normal control hips at 90° and between 100° and 120° of flexion (p ranging from 0.010 to 0.039; Fig. 2B); eg, IR at 110° of flexion was increased in hips with a spherical head-neck morphology $33^\circ \pm 14^\circ$ (range, -7° to 41°) compared with the nondysplastic controls ($20^\circ \pm 16^\circ$; range, -7° to 41° ; $p = 0.010$; Fig. 2B). IR did not differ between hips with a cam-type morphology and the nondysplastic control hips with the numbers available (p ranging from 0.263 to 0.952; Fig. 2B).

Hips with a concomitant IO had increased ER in the posterior impingement test compared with hips without an IO (p ranging from 0.003 to 0.009; Fig. 2D); eg, ER at 0° of flexion in hips with a concomitant IO ($37^\circ \pm 7^\circ$; range, 21° – 41°) was increased compared with hips without an IO ($19^\circ \pm 19^\circ$; range, -10° to 41° ; $p = 0.008$; Fig. 2D). There was no difference in ER in hips with a concomitant IO compared with the nondysplastic control hips with the numbers available (p ranging from 0.383 to 0.777; Fig. 2D); eg, $37^\circ \pm 7^\circ$ (range, 21° – 41°) of ER in 0° of flexion in hips with concomitant IO compared with $38^\circ \pm 7^\circ$ (range, 17° – 41°) in nondysplastic control hips ($p = 0.777$; Fig. 2D).

Table 3. Results of ROM of the three study groups

Parameter	Dysplasia (preoperatively)	PAO (after PAO)	Normal	p value preoperative versus PAO	p value preoperative versus normal	p value PAO versus normal
Flexion (°)	148 ± 20 (97–171)	127 ± 19 (84–161)	128 ± 15 (107–159)	< 0.001	0.001	0.867
Extension (°)	24 ± 11 (–3 to 30)	19 ± 15 (–18 to 30)	28 ± 3 (19–30)	0.109	0.305	0.017
Internal rotation in 90° flexion (°)	39 ± 6 (14–41)	34 ± 14 (–10 to 41)	33 ± 9 (13–41)	0.059	0.001	0.151
External rotation in 0° flexion (°)	26 ± 18 (–10 to 41)	25 ± 18 (–10 to 41)	38 ± 7 (17–41)	0.592	0.009	0.002
Adduction (°)	41 ± 13 (5–61)	48 ± 14 (7–61)	54 ± 8 (29–61)	0.029	< 0.001	0.139
Abduction (°)	88 ± 4 (73–90)	57 ± 14 (22–75)	65 ± 10 (41–80)	< 0.001	< 0.001	0.061

Values are expressed as mean ± SD with ranges in parentheses; PAO = periacetabular osteotomy.

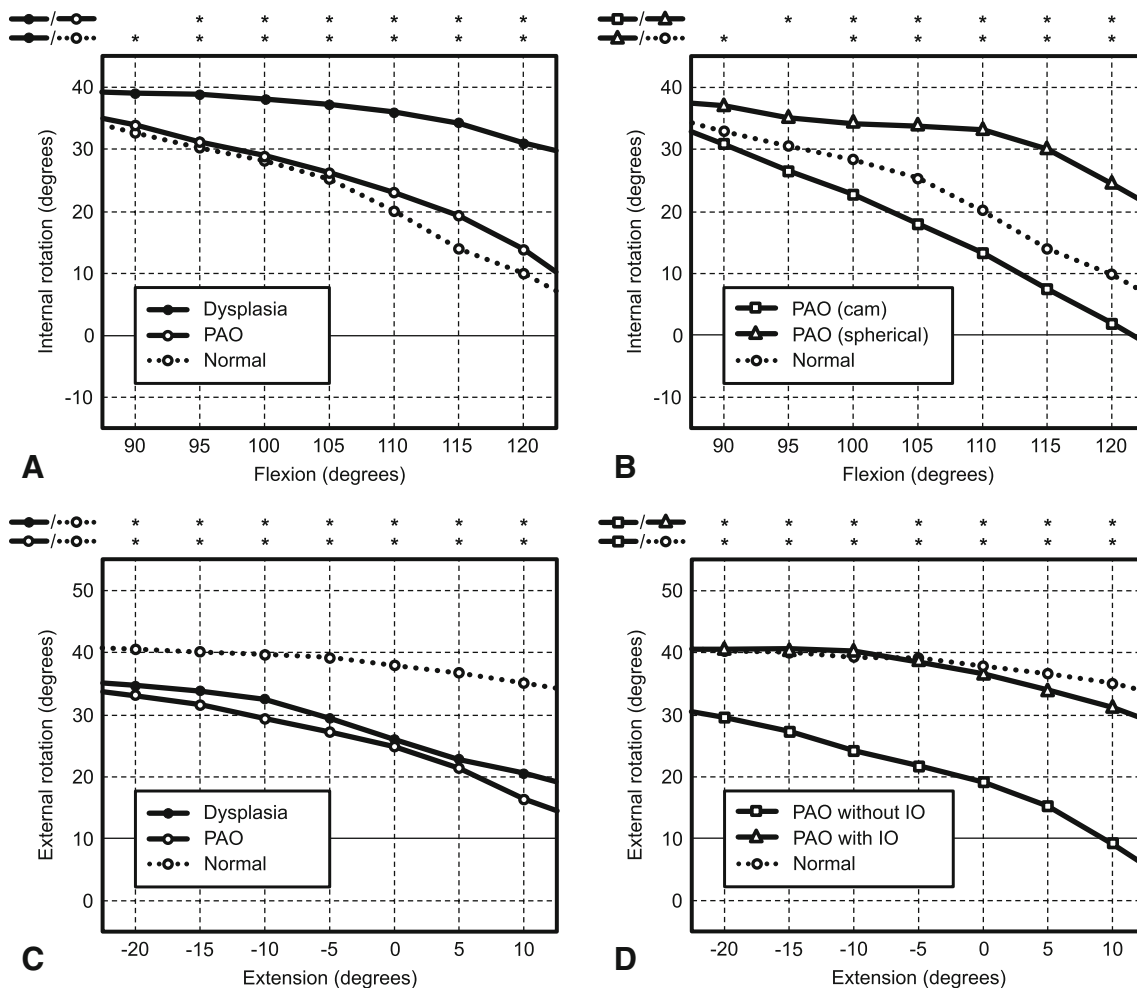


Fig. 2A–D Shown are the results of the anterior impingement test for (A) the three study groups and (B) PAOs with and without a cam-type morphology. The results of the posterior impingement test are shown

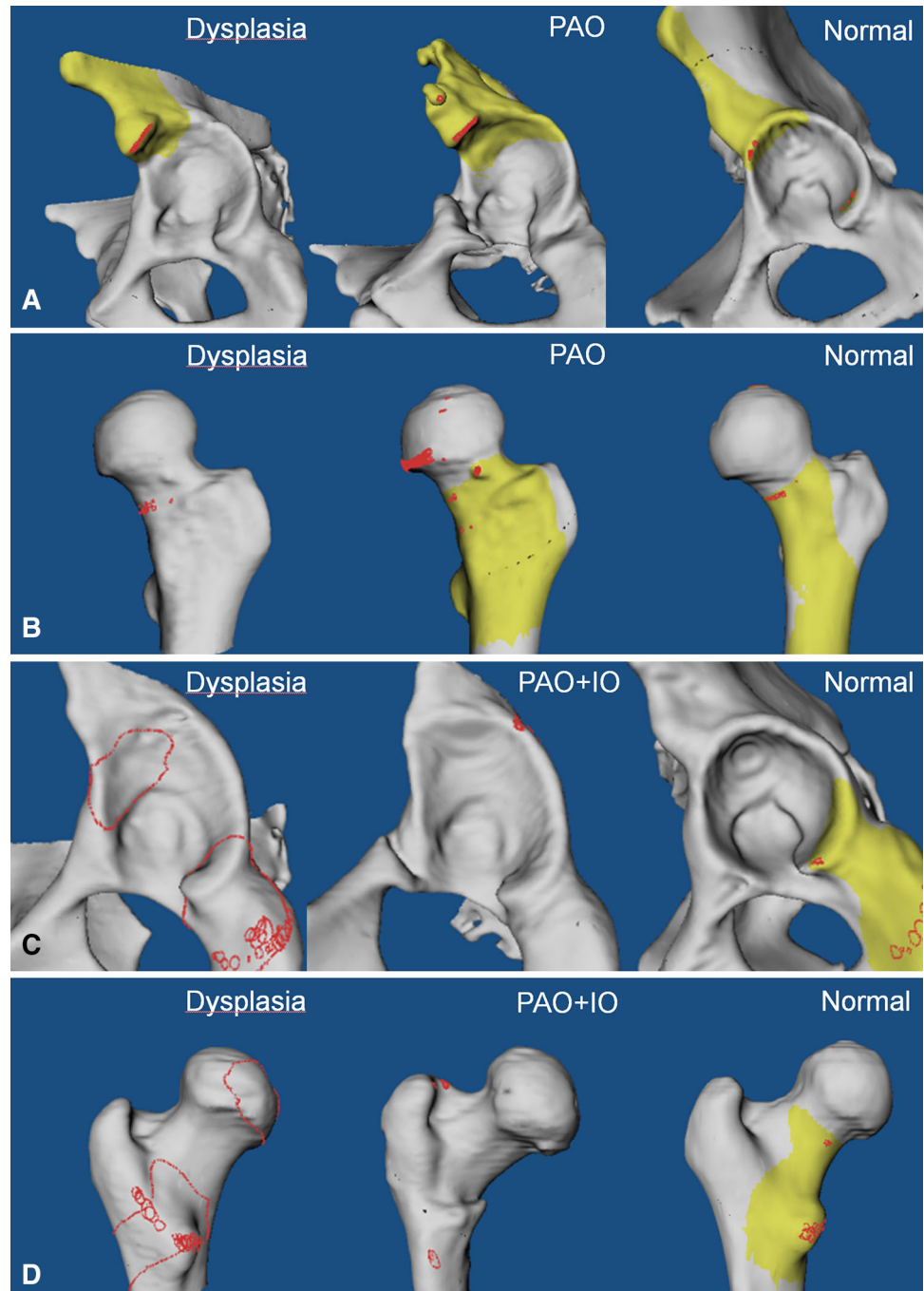
for (C) the three study groups and (D) PAOs with and without a concomitant IO. *Significant difference.

Discussion

Proximal femoral pathomorphologies often are present in hips with DDH. This includes an aspherical femoral head

and a valgus configuration with high antetorsion. Both pathomorphologies can result in painful restricted ROM after acetabular reorientation [1, 10, 28, 29]. An objective quantification of the resulting ROM after PAO for DDH is

Fig. 3A–D The impingement zones are given for the anterior impingement motion pattern for the (A) acetabular and the (B) femoral side for the three evaluated study groups. Similarly, the impingement zones are shown for the posterior impingement motion pattern for (C) the acetabular and the (D) femoral side.



difficult as a result of the lack of appropriate computer modeling methodology. In particular, the influence of a concomitant aspherical femoral head or a combined valgus and antetorsion deformity has never been investigated. With the help of a novel and sophisticated motion algorithm for complex hip deformities [17, 18, 25], we asked (1) if a PAO restores the typically excessive ROM in DDH compared with normal hips; (2) how impingement locations differ in dysplastic hips before and after PAO compared with normal hips; (3) if a cam-type morphology

of the proximal femur negatively affects IR in flexion after PAO for DDH; and (3) how a concomitant varus derotation IO affects ER in extension after PAO when a valgus morphology of the proximal femur with high antetorsion was present preoperatively.

This study has several limitations. The main limitation is a potential selection bias of including only 27 hips (14%) with a pre- and postoperative CT scan allowing computer simulation of ROM. The majority of patients during the study period of January 1999 to March 2002 did not have

Table 4. Distribution of impingement locations for the two evaluated motion patterns (anterior and posterior impingement test) for the three study groups

Parameter	Dysplasia (preoperatively)	Dysplasia (after PAO)	Normal	p value preoperative versus PAO	p value preoperative versus normal	p value PAO versus normal
Anterior impingement test						
Acetabular rim	78% (21/27)	82% (22/27)	100% (19/19)	0.5	0.032	0.059
Lunate surface	26% (7/27)	44% (12/27)	42% (8/19)	0.127	0.202	0.558
Anteroinferior iliac spine	48% (13/27)	59% (16/27)	5% (1/19)	0.293	0.002	< 0.001
Supraacetabular	7% (2/27)	0% (0/27)	0% (0/19)	0.245	0.339	1
Ischium	0% (0/27)	0% (0/27)	0% (0/19)	1	1	1
Femoral head	30% (8/27)	59% (16/27)	53% (10/19)	0.027	0.103	0.773
Femoral neck	15% (4/27)	30% (8/27)	5% (1/19)	0.163	0.302	0.043
Femoral head-neck junction	93% (25/27)	93% (25/27)	100% (19/19)	0.695	0.339	0.339
Greater trochanter	0% (0/27)	0% (0/27)	0% (0/19)	1	1	1
Lesser trochanter	0% (0/27)	7% (2/27)	0% (0/19)	0.245	1	0.339
Intertrochanteric crest	0% (0/27)	0% (0/27)	0% (0/19)	1	1	1
Femoral shaft	7% (2/27)	22% (6/27)	21% (4/19)	0.125	0.182	0.61
Posterior impingement test						
Acetabular rim	22% (6/27)	44% (12/27)	84% (16/19)	0.074	< 0.001	0.007
Lunate surface	44% (12/27)	44% (12/27)	0% (0/19)	0.608	< 0.001	< 0.001
Anteroinferior iliac spine	0% (0/27)	0% (0/27)	0% (0/19)	1	1	1
Supraacetabular	0% (0/27)	4% (1/27)	0% (0/19)	0.5	1	0.589
Ischium	85% (23/27)	96% (26/27)	100% (19/19)	0.175	0.108	0.587
Femoral head	26% (7/27)	41% (11/27)	5% (1/19)	0.193	0.073	0.007
Femoral neck	26% (7/27)	4% (1/27)	0% (0/19)	0.025	0.017	0.587
Femoral head-neck junction	22% (6/27)	19% (5/27)	79% (15/19)	0.5	< 0.001	< 0.001
Greater trochanter	19% (5/27)	59% (16/27)	0% (0/19)	0.002	0.059	< 0.001
Lesser trochanter	89% (24/27)	85% (23/27)	95% (18/19)	0.5	0.448	0.302
Intertrochanteric crest	78% (21/27)	89% (24/27)	58% (11/19)	0.234	0.132	0.019
Femoral shaft	7% (2/27)	4% (1/27)	5% (1/19)	0.5	0.632	0.661

Values are expressed as percentage with absolute numbers in parentheses; PAO = periacetabular osteotomy.

pre- and postoperative CT scans (142 hips) or were excluded because the scans were not suitable for computer simulation (31 hips). Although the demographic factors between the study population and the excluded hips did not differ, a potential selection bias cannot be entirely excluded. However, the current study population potentially represents valuable information because it includes the maximum number of hips available with suitable CT imaging for computer-simulated ROM. The MRI has become today's standard 3-D imaging in PAO, but it does not yet allow simulation of hip ROM using a modern motion algorithm. Second, our computerized evaluation of ROM only detects bony abutment and does not take into account the soft tissues. This is a well-known limitation for computer simulation of hip ROM [6, 12, 25]. Our values for hip ROM are comparable with other computer motion analyses [6, 12]. Because both the anterior and the posterior impingement motion patterns are mainly restricted

by bony abutment, however [7, 20, 24, 25], this limitation should not compromise our findings. However, future clinical studies are needed to confirm the results of the current study. Third, we used the anteroinferior iliac spine to reconstruct the APP as a reference plane. However, our results for ROM in the dysplasia and normal group match well with those found in the literature [6, 7, 20, 24, 25]. In addition, because we used the same reconstructed APP pre- and postoperatively for each patient, the evaluated comparisons should not be compromised. Next, the normal group was notably older and had an increased percentage of male patients compared with the PAO group (Table 1). The difference in age was the result of the fact that patients eligible for joint-preserving surgery are younger than patients with a THA (normal hips were recruited from the contralateral side of patients with CT-based navigated THA). This should not have jeopardized our results. In contrast, if the anatomy of a hip does not result in any signs

Table 5. Selected literature on range of motion after acetabular osteotomies for hip dysplasia

Study	Surgery	Method	Number of hips	Flexion (°)		Internal rotation in 90° of flexion (°)	
				Preoperative	Postoperative	Preoperative	Postoperative
Steppacher et al. [21]	PAO	Clinical	75	117 ± 13 (90–130)	100 ± 11 (80–130)*	41 ± 14 (20–70)	32 ± 15 (0–60)*
Ziebarth et al. [29]	PAO	Clinical	46	100 ± 11 (60–120)	95 ± 10 (50–115)*	28 ± 16 (0–60)	22 ± 13 (0–50)*
Albers et al. [1]	PAO [†]	Clinical	122	112 ± 15 (90–140)	99 ± 11 (70–120)*	28 ± 19 (–50 to 70)	22 ± 15 (0–45)
Ninomiya [14]	PAO [‡]	Clinical	43	112 ± 18 (80–140)	101 ± 12 (80–130)*	26 ± 16 (–10 to 70)	19 ± 14 (0–60)*
Nakamura et al. [13]	RAO	Clinical	41	118 ± 15 (80–140)	110 ± 21 (60–140)	–	–
Hasegawa et al. [5]	RAO	Clinical	145	118 (75–145)	98 (10–140)	–	–
Iwai et al. [6]	RAO	Clinical	273	112 (50–135)	110 (30–140)	–	–
Current study	RAO	Computer	12	133 ± 11 (117–153)	106 ± 13 (85–122)*	55 ± 30 (24–87)	25 ± 18 (0–52)*
	PAO	Computer	27	148 ± 20 (97–171)	127 ± 19 (84–161)*	39 ± 6 (14 to 41)	34 ± 14 (–10 to 41)

Study	External rotation in 0° or 90° of flexion (°)		Abduction (°)		Results
	Preoperative	Postoperative	Preoperative	Postoperative	
Steppacher et al. [21]	35 ± 15 (0–70)	17 ± 12 (0–40)*	38 ± 10 (20–60)	33 ± 9 (20–50)*	Flexion, internal and external rotation, and abduction decreased
Ziebarth et al. [29]	–	–	31 ± 7 (20–50)	28 ± 6 (10–45)*	Flexion, internal rotation, and abduction decreased
Albers et al. [1]	38 ± 11 (–20 to 15)	33 ± 12 (0–15)	39 ± 12 (10–80)	37 ± 12 (10–70)	Flexion decreased in both groups ^{†,‡} ; internal and external rotation decreased and extension increased in PAOs with suboptimal
	39 ± 15 (–10 to 20)	30 ± 17 (0–30)*	38 ± 11 (10–60)	34 ± 12 (0–60)	acetabular orientation and/or offset
Ninomiya [14]	–	–	29 ± 15 (15–45)	24 ± 10 (5–50)	Flexion and abduction decreased
Nakamura et al. [13]	–	–	27 (10–60)	20 (–5 to 50)	Flexion and abduction decreased
Hasegawa et al. [5]	–	–	28 (0–45)	26 (0–45)	No changes in flexion or abduction
Iwai et al. [6]	35 ± 15 (4–55) [§]	40 ± 14 (20–53) [§]	63 ± 26 (21–84)	49 ± 14 (34–81)*	Flexion, internal rotation, and abduction decreased
Current study	26 ± 18 (–10 to 41) [§]	25 ± 18 (–10 to 41) [§]	88 ± 4 (73–90)	57 ± 14 (22–75)*	Flexion and abduction decreased; adduction increased; internal rotation decreased at > 90° of flexion

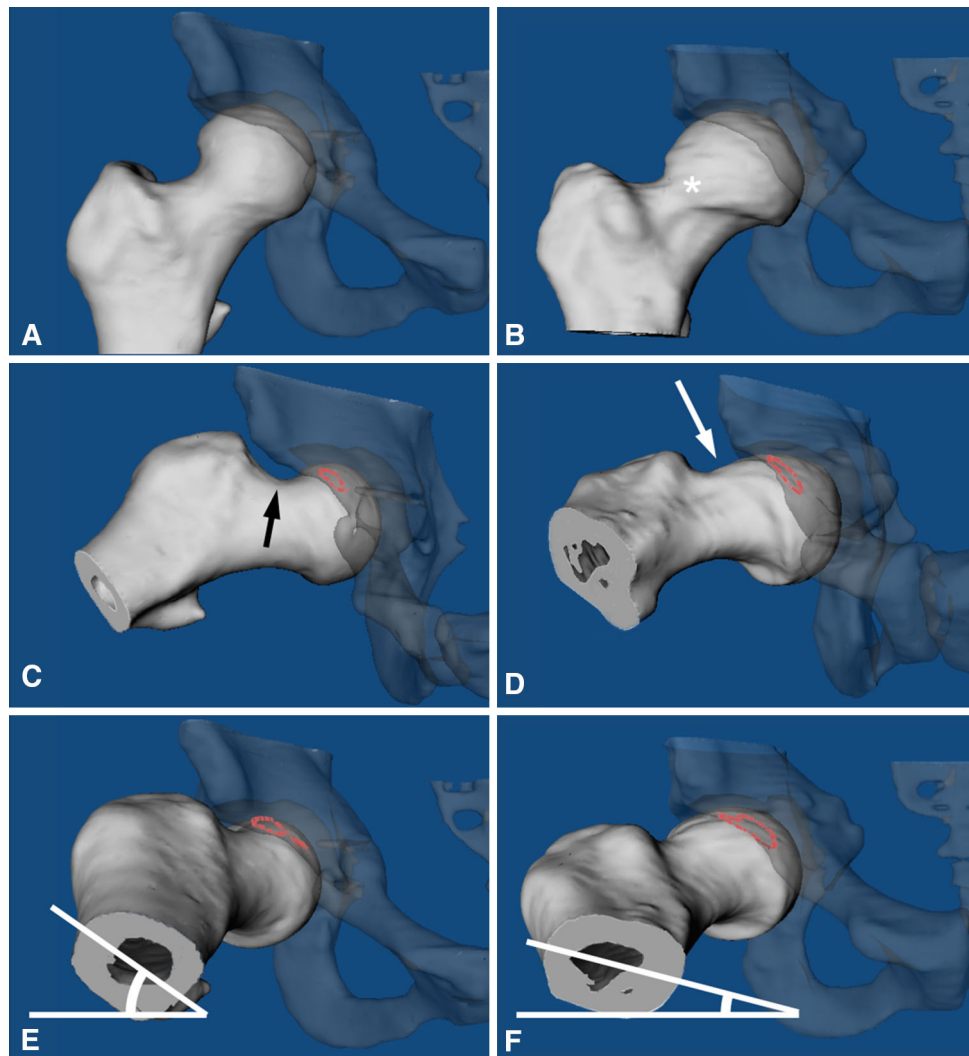
Values are expressed as mean ± SD with ranges in parentheses; *significant difference compared to preoperative status reported in the literature; [†]optimal acetabular orientation and femoral offset; [‡]suboptimal acetabular orientation and/or femoral offset; [§]external rotation in 0° of flexion; PAO = periacetabular osteotomy; RAO = rotational acetabular osteotomy.

of osteoarthritis at a mean age of 54 years (normal group; Table 1), a relevant pathomorphology resulting in early osteoarthritis in this asymptomatic control group can basically be excluded. The difference in sex distribution is attributable to the fact that hip dysplasia is more common in females. In addition, a concomitant IO was not consistently performed in hips with a CCD angle $> 135^\circ$ or a femoral antetorsion $> 25^\circ$ but only in hips with a positive apprehension test. Therefore, there is some overlap for the CCD angle or femoral antetorsion between hips with and without a concomitant IO (Table 2). Nevertheless, ER differed significantly between these two subgroups (Fig. 2D). Finally, we did not evaluate the effect of pelvic orientation, which can also affect hip ROM (eg, decreased flexion with increasing pelvic tilt).

Comparing our computed ROM in dysplastic hips after PAO with the clinical results reported by others, flexion [1, 21, 29], IR in 90° of flexion [1, 21, 29], and abduction [21, 29] were decreased after PAO (Table 5). In contrast, no

difference for flexion [5, 13, 14] and abduction [5, 13, 14] were found in hips after a rotational acetabular osteotomy (Table 5). We found no difference in ER in 0° of flexion after PAO, whereas in clinical studies measuring external rotation in 90° of flexion, ER was seen to decrease [1, 21] (Table 5; Fig. 2C). Only one study is available that computed the virtual ROM after pelvic osteotomy for DDH [6]. In contrast to our method, a motion algorithm with a single center of rotation was used. Inherently, this resulted in a different ROM in dysplastic hips with decreased flexion and abduction and increased IR and ER (Table 5). Nevertheless, the tendencies for postoperative changes in these motions were consistent with our method. In comparison to previous studies with clinical [1, 5, 13, 14, 21, 29] measurement of ROM in hips with PAO, the method in the current study had the following advantages: more accurate and anatomically based quantification of ROM because clinical assessment is subject to error [2], the identification of motion patterns (anterior and posterior impingement test) instead of isolated

Fig. 4A–F The 3-D CT-based surface models of (A) a dysplastic hip with a spherical femoral head and (B) a dysplastic hip with a cam-type morphology (asterisk) both after PAO are shown. Anterosuperior head-neck offset was (C) normal in the hip with a spherical femoral head and (D) substantially decreased in the hip with a cam-type morphology. ROM was evaluated using computerized methods. (E) Hips with a spherical head showed increased IR (angle) in flexion compared with (F) hips with a cam-type morphology of the proximal femur.



amplitudes of ROM and the detection of the corresponding acetabular and femoral impingement zones.

In agreement with a previous report [11], we found a higher prevalence of extraarticular impingement for the dysplastic hips. More specifically, the anteroinferior iliac spine can become more problematic after the acetabular reorientation (Fig. 3A). In addition, the PAO increases the prevalence of intraarticular impingement of the aspherical femoral head (Fig. 3B). An additional varus derotation osteotomy of the proximal femur can decrease the extraarticular impingement in extension and external rotation (Fig. 3C–D), similar to what had been shown for nondysplastic hips [20].

We found decreased IR for the anterior impingement test in hips with a cam-type morphology compared with hips with a spherical femoral head (Fig. 4). There were no differences in the acetabular reorientation, the CCD angle, or the femoral antetorsion between the spherical and the aspherical subgroups (Table 2). Therefore, the decreased IR in 90° of flexion can most likely be attributed to the anterosuperior femoral head asphericity (Fig. 2B). These results from virtual simulation of ROM confirm independently the risk of femoroacetabular impingement after PAO [1, 10, 29]. An aspherical femoral head-neck in a dysplastic hip is compensated for by the deficient acetabular coverage. After PAO with increased acetabular coverage, the asphericity can become apparent resulting in an anterior impingement with decreased IR in flexion [1, 10, 29]. Clinical studies have suggested correcting this aspherical femoral head morphology after PAO to improve IR in flexion [1, 10, 29], which has been associated with an increased survivorship of the hip after PAO [1].

Even with nondysplastic acetabular morphology, a valgus hip with high antetorsion restricts ER in extension [20]. It has been shown that this is the result of extraarticular impingement between the proximal femur and the ischium [20]. This motion was classically described as a positive “apprehension test” in hips with DDH [27] and suggested that this posterior impingement conflict might act as a fulcrum that can aggravate the anterior instability. We showed that a varus and derotation IO is able to restore a normal hip motion pattern in extension and ER while maintaining normal flexion and IR. This can potentially decrease the posterior extraarticular conflict, which is often residually present in long-term followup after PAO without IO [1, 21]. The indication for this additional procedure needs to be weighed against its inherent morbidity and possible complications. It can theoretically be performed at a second stage if symptoms in extension and external rotation are persistent after the PAO.

In summary, the current study demonstrated that a PAO reduces the typically increased flexion, IR, and abduction in dysplastic hips compared with normal values. After acetabular reorientation, a cam-type morphology of the

proximal femur reduces flexion and IR and can lead to an anterior femoroacetabular intra- and extraarticular impingement conflict. The associated valgus neck-shaft angle with high antetorsion in dysplastic hips can result in restricted ER and posterior impingement. This motion can be normalized with a varus derotation IO.

Acknowledgments We thank Evgeny Bulat and Michelle Heinz (Department of Orthopaedic Surgery, Boston Children’s Hospital, Harvard Medical School, Boston, MA, USA) for their effort in collecting the clinical data of the patient series and the excluded patients after PAO during the study period. In addition, we appreciate the assistance of Patricia Miller (Department of Orthopaedic Surgery, Boston Children’s Hospital, Harvard Medical School, Boston, MA, USA) for the statistics.

References

- Albers CE, Steppacher SD, Ganz R, Tannast M, Siebenrock KA. Impingement Adversely affects 10-year survivorship after periacetabular osteotomy for DDH. *Clin Orthop Relat Res*. 2013;471:1602–1614.
- Charbonnier C, Chagué S, Schmid J, Kolo FC, Bernardoni M, Christofilopoulos P. Analysis of hip range of motion in everyday life: a pilot study. *Hip Int*. 2014 Nov 10 [Epub ahead of print].
- Ganz R, Klaue K, Vinh TS, Mast JW. A new periacetabular osteotomy for the treatment of hip dysplasias. Technique and preliminary results. *Clin Orthop Relat Res*. 1988;232:26–36.
- Goodman DA, Feighan JE, Smith AD, Latimer B, Buly RL, Cooperman DR. Subclinical slipped capital femoral epiphysis. Relationship to osteoarthritis of the hip. *J Bone Joint Surg Am*. 1997;79:1489–1497.
- Hasegawa Y, Masui T, Yamaguchi J, Kawabe K, Suzuki S. Factors leading to osteoarthritis after eccentric rotational acetabular osteotomy. *Clin Orthop Relat Res*. 2007;459:207–215.
- Iwai S, Kabata T, Maeda T, Kajino Y, Watanabe S, Kuroda K, Fujita K, Hasegawa K, Tsuchiya H. Three-dimensional kinetic simulation before and after rotational acetabular osteotomy. *J Orthop Sci*. 2014;19:443–450.
- Kubiak-Langer M, Tannast M, Murphy SB, Siebenrock KA, Langlotz F. Range of motion in anterior femoroacetabular impingement. *Clin Orthop Relat Res*. 2007;458:117–124.
- Mahaisavariya B, Sitthiseripratip K, Tongdee T, Bohez EL, Vander Sloten J, Oris P. Morphological study of the proximal femur: a new method of geometrical assessment using 3-dimensional reverse engineering. *Med Eng Phys*. 2002;24:617–622.
- Murphy SB, Simon SR, Kijewski PK, Wilkinson RH, Griscom NT. Femoral anteversion. *J Bone Joint Surg Am*. 1987;69:1169–1176.
- Myers SR, Eijer H, Ganz R. Anterior femoroacetabular impingement after periacetabular osteotomy. *Clin Orthop Relat Res*. 1999;363:93–99.
- Nakahara I, Takao M, Sakai T, Miki H, Nishii T, Sugano N. Three-dimensional morphology and bony range of movement in hip joints in patients with hip dysplasia. *Bone Joint J*. 2014 96:580–589.
- Nakahara I, Takao M, Sakai T, Nishii T, Yoshikawa H, Sugano N. Gender differences in 3D morphology and bony impingement of human hips. *J Orthop Res*. 2011;29:333–339.
- Nakamura S, Ninomiya S, Takatori Y, Morimoto S, Umeyama T. Long-term outcome of rotational acetabular osteotomy: 145 hips followed for 10–23 years. *Acta Orthop Scand*. 1998;69:259–265.

14. Ninomiya S. Rotational acetabular osteotomy for the severely dysplastic hip in the adolescent and adult. *Clin Orthop Relat Res.* 1989;247:127–137.
15. Noble PC, Kamaric E, Sugano N, Matsubara M, Harada Y, Ohzono K, Paravic V. Three-dimensional shape of the dysplastic femur: implications for THR. *Clin Orthop Relat Res.* 2003;417:27–40.
16. Nötzli HP, Wyss TF, Stoecklin CH, Schmid MR, Treiber K, Hodler J. The contour of the femoral head-neck junction as a predictor for the risk of anterior impingement. *J Bone Joint Surg Br.* 2002;84:556–560.
17. Puls M, Ecker TM, Steppacher SD, Tannast M, Siebenrock KA, Kowal JH. Automated detection of the osseous acetabular rim using three-dimensional models of the pelvis. *Comput Biol Med.* 2011;41:285–291.
18. Puls M, Ecker TM, Tannast M, Steppacher SD, Siebenrock KA, Kowal JH. The Equidistant Method—a novel hip joint simulation algorithm for detection of femoroacetabular impingement. *Comput Aided Surg.* 2010;15:75–82.
19. Reynolds D, Lucas J, Klaue K. Retroversion of the acetabulum. A cause of hip pain. *J Bone Joint Surg Br.* 1999;81:281–288.
20. Siebenrock KA, Steppacher SD, Haefeli PC, Schwab JM, Tannast M. Valgus hip with high antetorsion causes pain through posterior extraarticular FAI. *Clin Orthop Relat Res.* 2013;471:3774–3780.
21. Steppacher SD, Tannast M, Ganz R, Siebenrock KA. Mean 20-year followup of Bernese periacetabular osteotomy. *Clin Orthop Relat Res.* 2008;466:1633–1644.
22. Steppacher SD, Tannast M, Werlen S, Siebenrock KA. Femoral morphology differs between deficient and excessive acetabular coverage. *Clin Orthop Relat Res.* 2008;466:782–790.
23. Sugano N, Noble PC, Kamaric E, Salama JK, Ochi T, Tullos HS. The morphology of the femur in developmental dysplasia of the hip. *J Bone Joint Surg Br.* 1998;80:711–719.
24. Tannast M, Hanke M, Ecker TM, Murphy SB, Albers CE, Puls M. LCPD: reduced range of motion resulting from extra- and intra-articular impingement. *Clin Orthop Relat Res.* 2012;470:2431–2440.
25. Tannast M, Kubiak-Langer M, Langlotz F, Puls M, Murphy SB, Siebenrock KA. Noninvasive three-dimensional assessment of femoroacetabular impingement. *J Orthop Res.* 2007;25:122–131.
26. Tannast M, Röthlisberger M, Gathmann S, Steppacher SD, Murphy SB, Langlotz F, Siebenrock KA. The interrelationship among different reference coordinate systems of the pelvis—a computer-assisted anatomical study. In: Davies BL, Joskowicz L, Leung KS, eds. *Computer Assisted Orthopaedic Surgery.* Berlin, Germany: Pro Business; 2008:185–188.
27. Tannast M, Siebenrock KA, Anderson SE. Femoroacetabular impingement: radiographic diagnosis—what the radiologist should know. *AJR Am J Roentgenol.* 2007;188:1540–1552.
28. Tönnis D, Heinecke A. Acetabular and femoral anteversion: relationship with osteoarthritis of the hip. *J Bone Joint Surg Am.* 1999;81:1747–1770.
29. Ziebarth K, Balakumar J, Domayer S, Kim YJ, Millis MB. Bernese periacetabular osteotomy in males: is there an increased risk of femoroacetabular impingement (FAI) after Bernese periacetabular osteotomy? *Clin Orthop Relat Res.* 2011;469:447–453.